

Room-temperature InAs_{0.89}Sb_{0.11} photodetectors for CO detection at 4.6 μm

H. H. Gao and A. Krier^{a)}

Physics Department, Lancaster University, Lancaster, LA1,4YB United Kingdom

V. V. Sherstnev

Ioffe Physico-Technical Institute, Polytechnicheskaya 26, St. Petersburg 194022, Russia

(Received 15 March 2000; accepted for publication 13 June 2000)

An InAs_{0.89}Sb_{0.11} photovoltaic detector that operates at room temperature in the 2.5–5 μm mid-infrared wavelength region is reported. The photodiode has an extended spectral response compared with other currently available III–V room-temperature detectors. In order to accommodate the large lattice mismatch between the InAs_{0.89}Sb_{0.11} active region and the InAs substrate, a buffer layer with an intermediate composition was introduced into the structure. In this way, we obtained room-temperature photodiodes with a cutoff wavelength near 5 μm , a peak responsivity of 0.8 A/W, and a detectivity of $1.26 \times 10^9 \text{ cm Hz}^{1/2}/\text{W}$. These devices could be effectively used as the basis of an optical sensor for the environmental monitoring of carbon monoxide at 4.6 μm , or as a replacement for PbSe photoconductors. © 2000 American Institute of Physics. [S0003-6951(00)02332-9]

Infrared photodetectors operating in the range 2–5 μm have wide ranging applications and are especially important as the key components in gas sensor instrumentation based on optical absorption.^{1,2} In particular, there is a need for efficient and reliable semiconductor light sources and detectors, which can be used for CO detection at 4.6 μm . Currently, the dominant infrared detector materials appropriate for this application are PbSe, HgCdTe, and InSb. However, both PbSe and HgCdTe are normally used in the photoconductive mode, PbSe has a relatively slow response speed which limits the modulation frequency and the integration time of the final gas sensor instrument. PbSe also suffers from undesirable $1/f$ noise problems, while HgCdTe normally requires thermoelectric cooling below room temperature in order to achieve a sufficiently high detectivity for successful instrumentation. Recent developments in HgCdTe have resulted in a D^* in excess of $2.5 \times 10^9 \text{ cm Hz}^{1/2} \text{ W}^{-1}$ at 300 K in the 7–11 μm range.³ Photovoltaic InSb, on the other hand, is faster and can operate out to 5 μm , but requires cryogenic cooling to 77 K in order to obtain satisfactory diode performance. Such factors significantly restrict the use of these detectors in portable gas detection systems, infrared spectrometers, thermal imaging cameras, and other applications where the need to provide cooling of the detector element makes the overall system cumbersome. Clearly there is a need for a fast photovoltaic detector operating at room temperature beyond 4 μm . Such a photodetector would be a major advantage and would have wide ranging applications.

The InAs_{1-x}Sb_x ternary alloy is potentially a more promising material for mid-infrared optoelectronic devices. Recently a number of different approaches and growth techniques including molecular beam epitaxy,^{4,5} metalorganic vapor phase epitaxy,^{6,7} and liquid phase epitaxy (LPE)^{8–10} have been investigated. One of the main obstacles in the development of InAs_{1-x}Sb_x devices is the preparation of

high quality epitaxial layers of appropriate composition on InAs substrates. The epitaxial growth of alloys with $x > 0.05$ directly on InAs leads to high concentrations of Shockley–Read recombination centers which limit the device quantum efficiency. However, we have found that it is possible to overcome this problem and recently we have reported efficient 4.6 μm light emitting diodes with output powers in excess of 1 mW operating at room temperature.¹¹ In this work, we now turn our attention to the corresponding detector and demonstrate an InAs_{0.89}Sb_{0.11} photodiode which operates at room temperature in the 2.5–5 μm mid-infrared wavelength range. This was achieved through introducing an intermediate composition buffer layer (InAs_{0.94}Sb_{0.06}) between the InAs substrate and the InAs_{0.89}Sb_{0.11} active region to relieve strain caused by the lattice mismatch. The detector has an extended spectral response out to longer wavelengths compared with currently available room-temperature detectors and is therefore well-suited to CO detection as well as other gas and flame monitoring applications.

The schematic energy band diagram of the double heterostructure InAs_{0.89}Sb_{0.11}/InAs_{0.55}Sb_{0.15}P_{0.30} photodiode is shown in Fig. 1. The epitaxial layers were grown by LPE at $\sim 545^\circ\text{C}$ using a conventional horizontal sliding graphite boat in an ultrapure hydrogen atmosphere. S-doped (100) n -type InAs substrates were used with a carrier concentration of $2 \times 10^8 \text{ cm}^{-3}$. The precursors for the growth melts were undoped polycrystalline InAs, InSb, InP, and 99.99999% pure indium metal. The p -type InAs_{0.55}Sb_{0.15}P_{0.30} was doped to $4 \times 10^{18} \text{ cm}^{-3}$ with Zn, whereas the n -type InAs_{0.55}Sb_{0.15}P_{0.30} layer was unintentionally doped and had a residual carrier concentration of $1 \times 10^{17} \text{ cm}^{-3}$. In order to remove impurities from the InAs_{0.89}Sb_{0.11} active region, this melt was baked out for 20 h at 750°C before the other melts were loaded into the boat. Then, to purify it still further, a little Gd (0.002 mol %) was added to the active region melt to act as an impurity gettering agent.^{12,19} Hall measurements revealed that this procedure reduced the residual carrier concentration in the active region to $< 2 \times 10^{16} \text{ cm}^{-3}$.

^{a)}Electronic mail: a.krier@lancaster.ac.uk

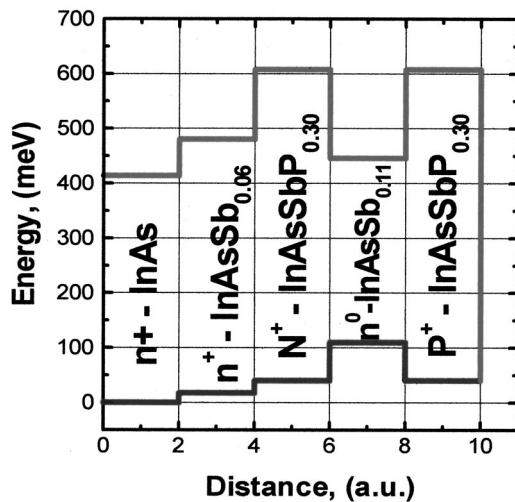


FIG. 1. A schematic energy band diagram showing the layer structure of the photodiode with an intermediate composition $\text{InAs}_{0.94}\text{Sb}_{0.06}$ buffer layer.

In order to relieve the misfit dislocation density in the active region due to the large mismatch (0.7%) between the $\text{InAs}_{0.89}\text{Sb}_{0.11}$ and the InAs substrate, a single $4\text{-}\mu\text{m}$ -thick buffer layer with an intermediate composition of $\text{InAs}_{0.94}\text{Sb}_{0.06}$ (0.4% mismatch to InAs substrate) was introduced into the structure. We favored this single step strain relaxation approach rather than using a multilayer buffer because it simplified the growth procedure.¹³ The undoped $5\text{-}\mu\text{m}$ -thick $\text{InAs}_{0.89}\text{Sb}_{0.11}$ active layer (*i* region) was sandwiched between two ($3\text{-}\mu\text{m}$ -thick) $\text{InAs}_{0.55}\text{Sb}_{0.15}\text{P}_{0.30}$ cladding layers instead of using just a single heterostructure which we used in our previous work.¹⁴ The double heterostructure is used for carrier confinement in the active region and helps prevent the tendency for electron loss to the InAs substrate. Due to the higher band gap, the upper cladding layer also acts as an effective transparent window layer.

The resulting epitaxial positive-intrinsic-negative (*p-i-n*) structures were processed into $300\text{ }\mu\text{m}$ diam mesa-etched photodiodes using conventional photolithography and processing techniques. Ohmic contacts were formed by thermal evaporation of Au to provide ohmic dot contacts, and finally the chips were mounted onto To49 headers for testing. No attempt was made to passivate the surfaces or include an antireflection coating at this stage of our work and all subsequent results refer to uncoated, unpassivated detectors. The detectivity, D^* and spectral response were measured using a chopping frequency of 300 Hz and a blackbody temperature of 1100 K. The recorded spectrum was corrected for system response using a Heimann LHi-807-G11 pyroelectric detector with a flat response.

Figure 2 shows the 77 K and room-temperature current–voltage (*I*–*V*) characteristics measured from one of the *p-i-n* photodiodes fabricated in the present work. The reverse dark current of the photodiode at 0.05 V reverse bias was measured to be approximately 10 μA and 1.5 mA at 77 and 300 K, respectively. The higher dark current at room temperature is a result of the narrow energy band gap of the active region material in which diffusion current is typically the dominant current conduction mechanism near room temperature. The reverse breakdown voltage decreases from -10 to -0.4 V with increasing temperature as the diode

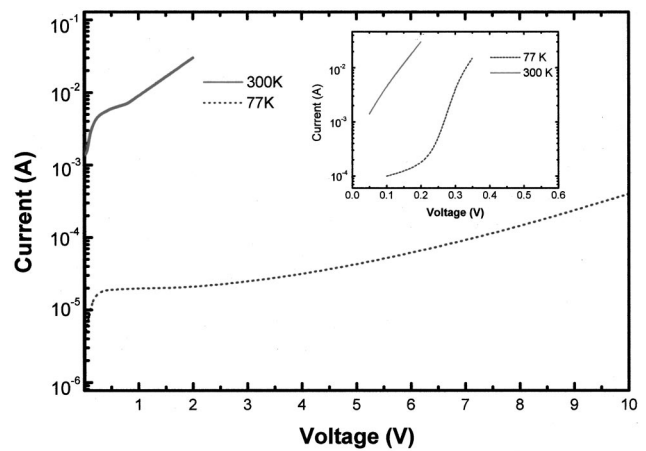


FIG. 2. A semilog plot of the photodiode *I*–*V* characteristics measured in reverse bias at 300 (solid line) and 77 K (dotted line). The forward bias characteristics are shown in the inset.

leakage current rises, which is quite a good result for an unpassivated photodiode in a narrow gap semiconductor. This value could be improved by using a structure with additional gating,¹⁵ but this was not attempted here. The diode diffusion equation was used to determine the energy band gap of the active region.¹⁶ A value of 0.267 eV was obtained, which is consistent with that calculated for an alloy composition of $\text{InAs}_{0.89}\text{Sb}_{0.11}$ at room temperature.¹⁷

The zero-bias resistance (R_0A) of the photodiode was obtained from the slope of the *I*–*V* characteristic near the origin. The R_0A product was plotted against $1/T$ for one of the $300\text{ }\mu\text{m}$ diameter photodiodes as shown in the semilog plot of Fig. 3. R_0A varies as $1/n_i^2$ and $1/n_i$ for the diffusion and generation-recombination mechanisms, respectively, where n_i is the intrinsic carrier concentration. As shown in Fig. 3, in the temperature range above 170 K, the R_0A product follows the diffusion model, whereas in the temperature range between 77 and 170 K, R_0A against T fits a generation-recombination model. This result is similar to our previous findings for $\text{In}_{0.97}\text{Ga}_{0.03}\text{As}/\text{InAs}_{0.36}\text{Sb}_{0.20}\text{P}_{0.44}$ $3.3\text{ }\mu\text{m}$ photodiodes.^{10,14} But, in the present case for these $4.6\text{ }\mu\text{m}$ photodiodes, the diffusion current remains dominant down to 170 K.

The room temperature photoresponse of the $\text{InAs}_{0.89}\text{Sb}_{0.11}$ photodiode is shown in Fig. 4. The effect of

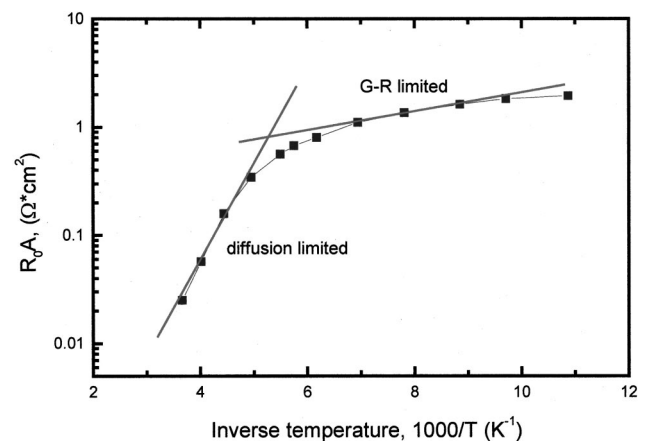


FIG. 3. The temperature dependence of the resistance area (R_0A) product for a typical $\text{InAs}_{0.89}\text{Sb}_{0.11}$ photodiode.

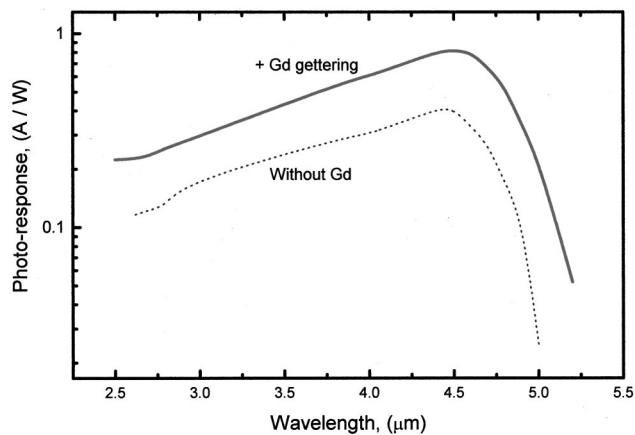


FIG. 4. The room-temperature photoresponse of the $\text{InAs}_{0.89}\text{Sb}_{0.11}$ photodiode obtained with Gd gettering (solid line) and without Gd gettering (dashed line) of the active region.

using Gd as a gettering agent to purify the active region is clearly evident. A significant improvement in the photodiode performance was obtained for the purified diode due to the removal of impurities from the active region and the corresponding reduction in residual carrier concentration from $\sim 10^{17}$ to $\sim 10^{16} \text{ cm}^{-3}$. These findings are in good agreement with our previous results for gettering in both LPE grown InAs epitaxial layers and InAsSb LEDs.^{18,19} Gong *et al.* have also observed similar improvements in shorter wavelength photodiodes.²⁰ A peak responsivity of 0.8 A/W was obtained at a wavelength of 4.6 μm , with a cutoff near 5 μm . In the detector with the purified active region the cutoff wavelength is increased a little, which is again consistent with the removal of shallow (donor) impurities from the active region.

The room temperature detectivity, D^* of the photodiode was calculated from the Johnson noise limited equation²¹ and was determined to be $1.26 \times 10^9 \text{ cm Hz}^{1/2}/\text{W}$ at 4.6 μm . The corresponding quantum efficiency was estimated to be 22% at this wavelength. The performance of the photodiodes made in our laboratory is compared with that of other commercially available photodetectors in Fig. 5. Clearly the

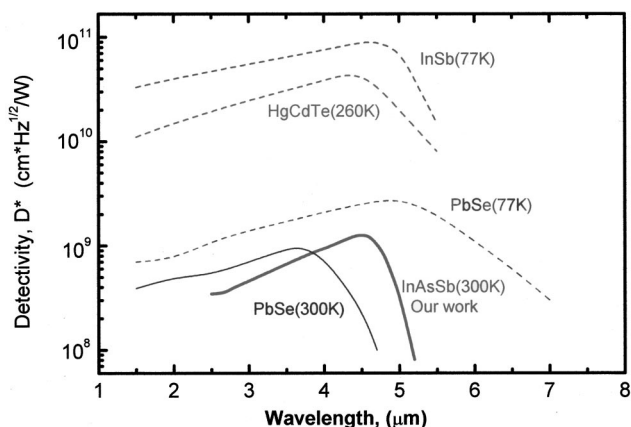


FIG. 5. A comparison of the spectral response of the $\text{InAs}_{0.89}\text{Sb}_{0.11}$ photodiodes of the present work and that of other commercially available photodetectors.

room-temperature cutoff wavelength is extended compared with PbSe. The room-temperature detectivity at 4.6 μm is approximately five times higher than that of a typical 300 K PbSe photoconductive detector at the same wavelength and is only three times lower than that of the 77 K PbSe detector. Only HgCdTe (260 K) and InSb (77 K) significantly outperform our photodiode but these need thermoelectric or liquid nitrogen cooling which makes them less attractive for practical applications.

In summary, an uncooled mid-infrared photodetector with a long cutoff wavelength has been made based on an $\text{InAs}_{0.89}\text{Sb}_{0.11}/\text{InAs}_{0.55}\text{Sb}_{0.15}\text{P}_{0.30}$ double heterostructure diode grown by LPE on an InAs substrate. Basic detector characteristics have been measured from unpassivated mesa-etched devices. The surface illuminated photodiodes exhibited a cutoff wavelength of $\sim 5 \mu\text{m}$ at room temperature, with a peak responsivity of 0.8 A/W and a Johnson-noise limited detectivity of $1.26 \times 10^9 \text{ cm Hz}^{0.5}/\text{W}$. Although some further optimization is required, we consider these devices to be a major step towards a LED-photodiode based CO gas sensor.

The authors wish to thank Kidde International for providing a studentship for H.H.G. They also wish to thank EPSRC for the award of a visiting fellowship for V.V.S.

- ¹ P. G. Eliseev, in *Semiconductor Optoelectronics*, edited by M. A. Herman (John Wiley & Sons, Chichester, 1980), p. 157.
- ² S. D. Smith, A. Vass, P. Bramley, J. G. Crowder, and C. H. Wang, *IEE Proc.: Optoelectron.* **144**, 266 (1997).
- ³ T. Ashley and N. T. Gordon, SPIE Conference, Photonics West meeting, San Jose, CA, January 1998, p. 3287.
- ⁴ A. Joulie, *J. Phys. IV* **9**, 79 (1999).
- ⁵ M. J. Pullin, H. R. Hardaway, J. D. Heber, C. C. Phillips, W. T. Yuen, R. A. Stradling, and P. Moeck, *Appl. Phys. Lett.* **74**, 2384 (1999).
- ⁶ B. Lane, D. Wu, A. Stein, J. Diaz, and M. Razeghi, *Appl. Phys. Lett.* **74**, 3438 (1999).
- ⁷ D. Wu, B. Lane, H. Mohseni, J. Diaz, and M. Razeghi, *Appl. Phys. Lett.* **74**, 1194 (1999).
- ⁸ I. A. Andreev, M. A. Afrailov, A. N. Baranov, M. P. Mikhailova, K. D. Moiseev, I. N. Timchenko, V. E. Shestnev, V. E. Umanski, and Y. P. Yakovlev, *Pis'ma Zh. Tekh. Fiz.* **16**, 27 (1990); *Tech. Phys. Lett.* **16**, 135 (1990).
- ⁹ B. Matveev, N. Zotova, S. Karandashov, M. Remennyi, N. Ilinskaya, N. Stus, V. Shustov, G. Talalakin, and J. Malinen, *IEE Proc.: Optoelectron.* **145**, 254 (1998).
- ¹⁰ A. Krier and Y. Mao, *Infrared Phys. Technol.* **38**, 397 (1997).
- ¹¹ A. Krier, H. H. Gao, V. V. Sherstnev, and Y. Yakovlev, *J. Phys. D* **32**, 3117 (1999).
- ¹² X. Y. Gong, H. Kan, T. Makino, T. Lida, Y. Z. Gao, M. Aoyama, M. Kumagawa, and T. Yamaguchi, *Jpn. J. Appl. Phys., Part 1* **38**, 685 (1999).
- ¹³ X. Y. Gong, T. Yamaguchi, H. Kan, T. Makino, N. L. Rowell, Y. Lacroix, A. Mangyou, R. Aoyama, and M. Kumagawa, *Jpn. J. Appl. Phys., Part 1* **36**, 738 (1997).
- ¹⁴ A. Krier, H. H. Gao, and Y. Mao, *Semicond. Sci. Technol.* **13**, 950 (1998).
- ¹⁵ R. M. Lin, S. F. Tang, S. C. Lee, C. H. Kuan, G. S. Chen, T. P. Sun, and J. C. Wu, *IEEE Trans. Electron Devices* **44**, 209 (1997).
- ¹⁶ S. M. Sze, *Physics of Semiconductor Devices* (Wiley, New York, 1969), Sec. 2.4.
- ¹⁷ H. H. Wieder and A. R. Clawson, *Thin Solid Films* **15**, 217 (1973).
- ¹⁸ A. Krier, H. H. Gao, and V. V. Sherstnev, *J. Appl. Phys.* **85**, 8419 (1999).
- ¹⁹ A. Krier, H. H. Gao, V. V. Sherstnev, and Y. Yakovlev, *J. Phys. D* **32**, 3117 (1999).
- ²⁰ X. Y. Gong, T. Yamaguchi, H. Kan, T. Makino, T. Lida, T. Kato, M. Aoyama, Y. Hayakawa, and M. Kumagawa, *Jpn. J. Appl. Phys., Part 1* **36**, 2614 (1997).
- ²¹ P. N. J. Dennis, *Photodetectors* (Plenum, New York, 1986).